Available online at www.sciencedirect.com
ScienceDirect
Journal of Sound and Vibration 309 (2008) 330–337
JOURNAL OF SOUND AND VIBRATION
www.elsevier.com/locate/jsvi

Short Communication

Chaotic motion of Van der Pol–Mathieu–Duffing system under bounded noise parametric excitation

Jiaorui Li[a,b,*], Wei Xu[a], Xiaoli Yang[a], Zhongkui Sun[a]

[a]*Department of Applied Math, Northwestern Polytechnical University, Xi'an 710072, PR China*
[b]*School of Statistics, Xi'an University of Finance & Economics, Xi'an 710061, PR China*

Received 26 August 2006; accepted 11 May 2007
Available online 19 September 2007

Abstract

The chaotic behavior of Van der Pol–Mathieu–Duffing oscillator under bounded noise is investigated. By using random Melnikov technique, a mean square criterion is used to detect the necessary conditions for chaotic motion of this stochastic system. The results show that the threshold of bounded noise amplitude for the onset of chaos in this system increases as the intensity of the noise in frequency increases, which is further verified by the maximal Lyapunov exponents of the system. The effect of bounded noise on Poincaré map is also investigated, in addition the numerical simulation of the maximal Lyapunov exponents.

1. Introduction

Parametric excitation nonlinear dynamic system with Van der Pol dampling and Duffing restoring force has been focused on in recently [1], the system is extensively applied in representing plenty of engineering structure. It is very important and useful to study the nonlinear dynamical behaviors of this system. In this paper, it would be interesting to consider the following Van der Pol–Mathieu–Duffing stochastic differential equation

$$\ddot{x} - \omega_0^2 x + \varepsilon[(\mu - \alpha x^2)\dot{x} + \gamma x \cos(\Omega_1 t)] + \beta x^3 = \varepsilon\sigma x\xi(t), \tag{1}$$

where $\beta > 0$ is nonlinear term, γ and Ω_1 are intensity and frequency of the periodic coefficient, respectively. $\xi(t)$ is a bounded noise to be described in Section 2. In Ref. [1], the two times asymptotic bifurcation of the parametric excitation nonlinear system under principal parametric resonance with Van der Pol dampling and Duffing restoring force has been studied. The behavior of deterministic Mathieu–Duffing system has been investigated extensively by many researchers. For instance, Luo [2,3] in 2003 investigated Mathieu–Duffing oscillator with a twin-well potential, in his work, the approximate criteria for the onset and destruction of a specified, primary resonant band of the Mathieu–Duffing oscillator was developed. Leslie Ng et al. [4,5]

*Corresponding author. Department of Applied Math, Northwestern Polytechnical University, Xi'an 710072, PR China. Tel.: +86 29 88495453; fax: +86 29 88494314.
E-mail address: Jiaoruili@xaufe.edu.cn (J. Li).

0022-460X/$ - see front matter © 2007 Published by Elsevier Ltd.
doi:10.1016/j.jsv.2007.05.027

investigated the Mathieu equation to which is added a cubic nonlinearity x^3 term using averaging method. However, all above work is due to a deterministic Mathieu–Duffing oscillator.

For stochastic Mathieu–Duffing oscillator, the present paper author investigated the maximal Lyapunov exponent and almost-sure stability by using multiple scales method in Ref. [6]. Liu et al. have studied the chaotic motion of Duffing oscillator under bounded noise parametric excitation by using stochastic Melnikov method in Ref. [7]. Chunbiao Gan has studied the noise-induced chaos and discuss the effect of noises on erosion of safe basin in the softening Duffing oscillator in Ref. [8].

In this paper, the chaotic motion of Van der Pol–Mathieu–Duffing system under bounded noise excitation is investigated by using stochastic Melnikov method. The Melnikov method was first applied by Holmes [9] to study a periodically forced Duffing oscillator with negative linear stiffness. Melnikov method was extended to study stochastic dynamical system by Frey and Simiu [10].

2. Bounded noise

A harmonic function with constant amplitude and random frequency and phases is called bounded noise, which can be expressed by mathematical presentation as [7]

$$\xi(t) = \sigma \cos(\Omega_2 t + \psi), \quad \psi = \delta B(t) + \Gamma, \tag{2}$$

where Ω_2 and δ are positive constants, $B(t)$ is a standard Wiener process, Γ is a random variable uniformly distribution in $[0,2\pi)$. $\xi(t)$ is a stationary random process in wide sense with zero mean. Its covariance function is

$$C_\xi(\tau) = \frac{\sigma^2}{2}\exp\left(-\frac{\delta^2|\tau|}{2}\right)\cos(\Omega_2\tau) \tag{3}$$

and its spectral density is

$$S_\xi(\omega) = \frac{(\sigma\delta)^2}{2\pi}\left(\frac{1}{4(\omega-\Omega_2)^2+\delta^4}+\frac{1}{4(\omega+\Omega_2)^2+\delta^4}\right). \tag{4}$$

The variance of the bounded noise is

$$C(0) = \frac{\sigma^2}{2} \tag{5}$$

which implies that the bounded noise has finite power. The shape of spectral density depends on Ω_2 and δ, while the bandwidth of the bounded noise mainly depends on δ. It is a narrow-band process when δ is small. It is easy to see that the sample function of the bounded noise is continuous and bounded which are required in the derivation of Melnikov function [7].

3. Random Melnikov technique

For $\varepsilon = 0$, Eq. (1) is regarded as an unperturbed system and can be written as

$$\begin{aligned} \dot{x} &= y, \\ \dot{y} &= \omega_0^2 x - \beta x^3. \end{aligned} \tag{6}$$

The system (6) is a Hamiltonian system with Hamiltonian function

$$H(x,y) = \frac{1}{2}\left(y^2 - \omega_0^2 x^2 + \frac{1}{2}\beta x^4\right) \tag{7}$$

and the potential function is

$$V(x,y) = \frac{1}{2}\left(-\omega_0^2 x^2 + \frac{1}{2}\beta x^4\right). \tag{8}$$

Through the analysis of system (6), one can see that there are three equilibrium points. $P_0(0,0)$ being hyperbolic saddle, which be connected by two homoclinic orbits

$$x_0(t) = \pm\sqrt{2/\beta}\omega_0 \operatorname{sech}(\omega_0 t), \quad y_0(t) = \mp\sqrt{2/\beta}\omega_0 \operatorname{sech}(\omega_0 t)\tanh(\omega_0 t). \tag{9}$$

$P_1\left(\sqrt{2/\beta}\omega_0, 0\right)$ and $P_2\left(-\sqrt{2/\beta}\omega_0, 0\right)$ being centers as shown in Fig. 1(a), the potential function of the system (6) are shown in Fig. 1(b) when $\omega_0 = 1.0$, $\beta = 0.5$.

Now let us apply the random Melnikov technique to study Van der Pol–Mathieu–Duffing system under bounded noise excitation, the motion of the system (1) is of the form

$$\begin{aligned} \dot{x} &= y, \\ \dot{y} &= \omega_0^2 x - \beta x^3 - \varepsilon[(\mu - \alpha x^2)y + \gamma x \cos(\Omega_1 t) - \sigma x \cos(\Omega_2 t + \psi)]. \end{aligned} \tag{10}$$

The random Melnikov process for system (10) can be obtained by using formula given by Wiggins in Ref. [11] as follows:

$$\begin{aligned} M(t_0) &= \int_{-\infty}^{\infty} -(\mu - \alpha x_0^2(t))y_0^2(t)\,\mathrm{d}t - \int_{-\infty}^{\infty} \gamma x_0(t)y_0(t)\cos(\Omega_1 t)\,\mathrm{d}t + \int_{-\infty}^{\infty} \sigma x_0(t)y_0(t)\xi(t+t_0)\,\mathrm{d}t \\ &= \frac{16\alpha\omega_0^3 - 20\beta\mu\omega_0}{15\beta^2} + Z(t_0) = I + Z(t_0), \end{aligned} \tag{11}$$

where

$$I = (16\alpha\omega_0^3 - 20\beta\mu\omega_0)/15\beta^2 \tag{12}$$

and

$$Z(t_0) = \int_{-\infty}^{\infty} \sigma x_0(t)y_0(t)\xi(t+t_0)\,\mathrm{d}t. \tag{13}$$

The first two integrals in Eq. (11) represent the mean of the Melnikov process due to damping force and periodic parametric excitation, and the last integral denotes the random portion of the Melnikov process due to bounded noise $\xi(t)$.

Consider the mean of random process $E[\xi(t)]$ is zero, one can get

$$E[M(t_0)] = (16\alpha\omega_0^3 - 20\beta\mu\omega_0)/15\beta^2, \tag{14}$$

where $E[\cdot]$ is an expectation operator. Eq. (14) gives a constant. That is to say in mean sense chaos never occurs in system (1). Now, let us consider if random Melnikov process (11) has simple zeros in mean-square sense. In this case, the impulse response function is

$$h(t) = x_0(t)y_0(t) = -\frac{2\omega_0^2}{\beta}\operatorname{sech}^2(\omega_0 t)\tanh(\omega_0 t) \tag{15}$$

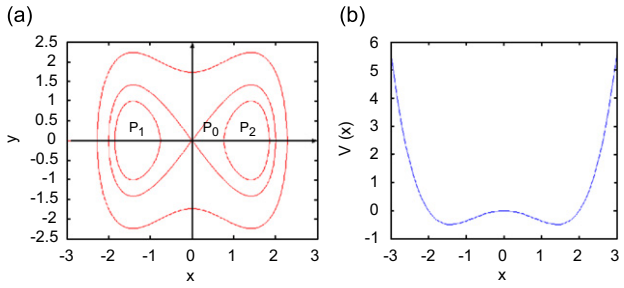

Fig. 1. Phase portrait and potential of system (6) for $\omega_0 = 1.0$, $\beta = 0.5$: (a) phase portrait and (b) potential.

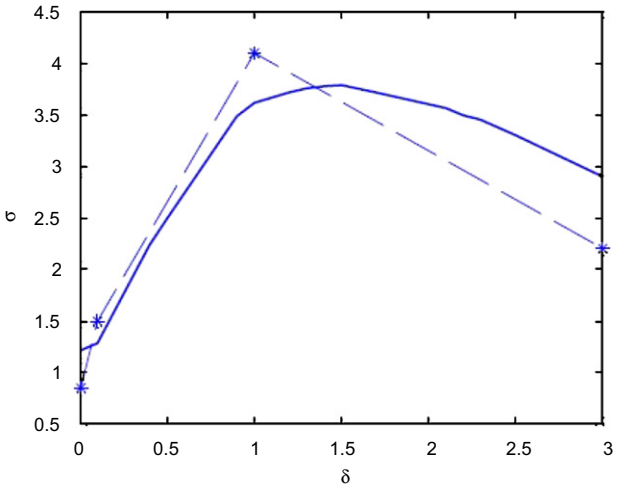

Fig. 2. The relation between δ and threshold σ ((—) analytic result, and (– – –) numerical result).

and the associated frequency response function is

$$H(\omega) = \int_{-\infty}^{\infty} h(t)\, \mathrm{e}^{-\mathrm{j}\omega t}\, \mathrm{d}t = \mathrm{j}\pi\omega^2 \mathrm{csch}(\pi\omega/4\omega_0)\mathrm{sech}(\pi\omega/4\omega_0)/2\beta. \tag{16}$$

The variance of $Z(t_0)$ as the output of the system can be expressed as follows:

$$\sigma_Z^2 = \int_{-\infty}^{\infty} |H(\omega)|^2 S_\xi(\omega)\, \mathrm{d}\omega. \tag{17}$$

The criterion for possible chaotic motion based on Melnikov process is performed in mean-square representation $I^2 = \sigma_Z^2$, i.e.

$$(16\alpha\omega_0^3/15\beta^2 - 4\mu\omega_0/3\beta^2) = \int_{-\infty}^{+\infty} [\mathrm{j}\pi\omega^2 \mathrm{csch}(\pi\omega/4\omega_0)\mathrm{sech}(\pi\omega/4\omega_0)/2\beta]^2 \frac{(\sigma\delta)^2}{2\pi} \left(\frac{1}{4(\omega-\Omega_2)^2+\delta^4} + \frac{1}{4(\omega+\Omega_2)^2+\delta^4} \right) \mathrm{d}\omega. \tag{18}$$

The integral in Eq. (18) can be calculated by numerical method. For the following parameter values: $\omega_0 = 1.0$, $\mu = 3.0$, $\alpha = 0.1$, $\beta = 1.0$, $\Omega_1 = \Omega_2 = 2.0$, one can get the threshold of bounded noise amplitude for onset of chaos in system (10) by numerical computation, which is shown in Fig. 2.

4. Numerical calculation

4.1. The largest Lyapunov exponent

The Lyapunov exponents characterize the asymptotic rate of exponential convergence or divergence of nearby orbits in phase space. Exponential divergence of nearby orbits implies that the behavior of a dynamical system is sensitive to initial conditions. A dynamical system with a positive largest Lyapunov exponent is usually a sign of chaos. To check the threshold of bounded noise amplitude for the onset of possible chaos, the largest Lyapunov exponent of system (1) is also calculated by the algorithm advanced by Wolf et al. [12]. For the following parameter values: $\omega_0 = 1.0$, $\varepsilon = 0.1$, $\mu = 3.0$ $\alpha = 0.1$, $\gamma = 6.0$, $\Omega_1 = 2.0$, $\beta = 1.0$, $\Omega_2 = 2.0$, the chaotic responses and the largest Lyapunov exponent of system (1) versus bounded noise amplitudes are shown in Fig. 3(a)–(d) for some different noise intensity values.

From Fig. 3, one can see that in the absence of noise and ω_0:Ω_1:Ω_2 = 1:2:2, the motion of the system (1) is chaotic for small noise amplitude, and noise amplitudes beyond the threshold value. Thus, there are many

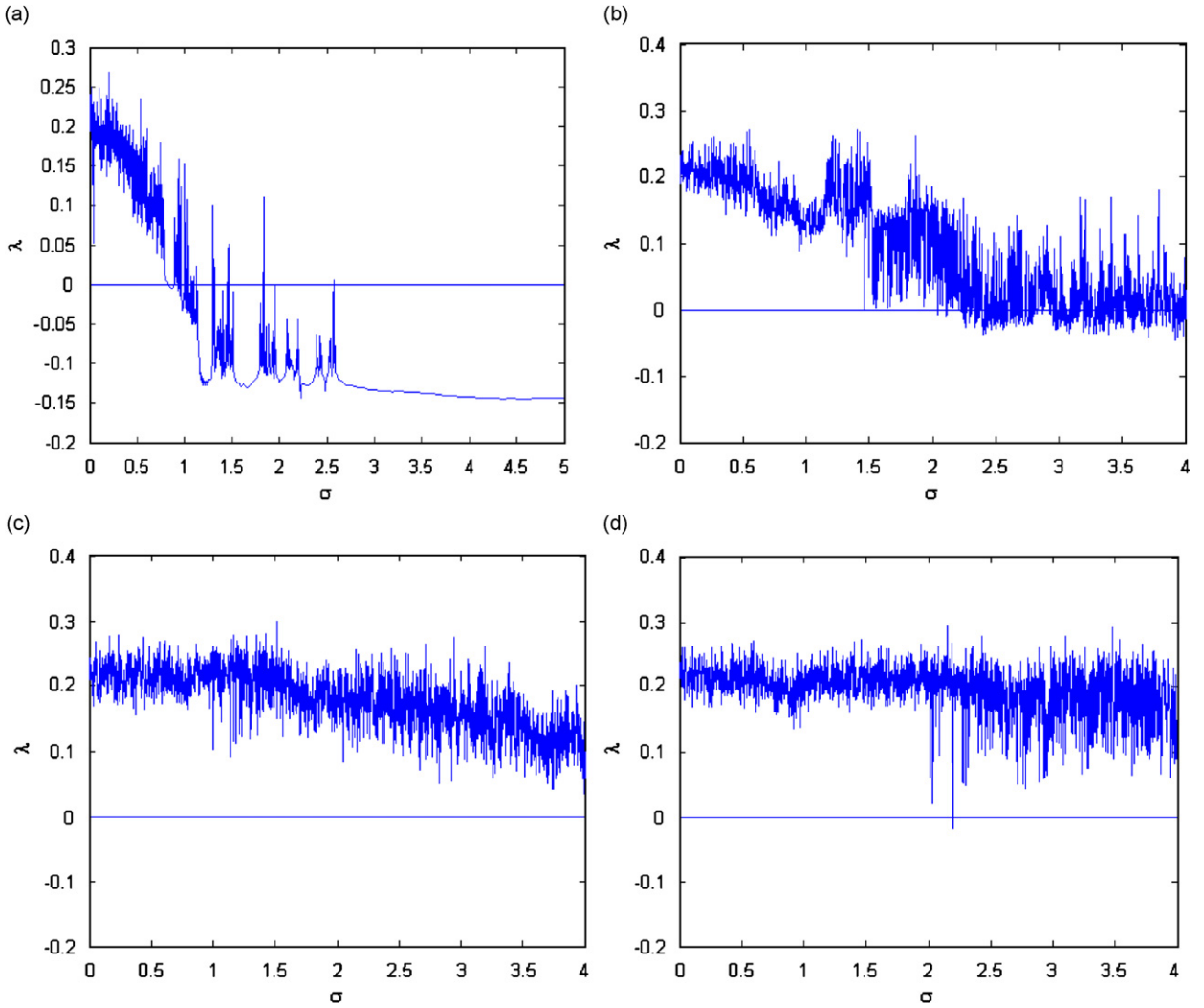

Fig. 3. The largest Lyapunov exponents of system (1) for different noise intensity values: (a) largest Lyapunov exponent ($\delta = 0$); (b) largest Lyapunov exponent ($\delta = 0.1$); (c) largest Lyapunov exponent ($\delta = 1.0$); and (d) largest Lyapunov exponent ($\delta = 3.0$).

intervals, in which λ becomes positive again and the response is periodic, by the increasing of noise amplitudes the motion of the system (1) is stable.

It is also seen from Fig. 3 that for the smaller noise intensity, i.e., $\delta \to 0$, the threshold σ for the onset of chaos decreases as the noise intensity δ increases.

4.2. Poincaré maps

Now we investigate system (1) by using its Poincaré maps. The Poincare map is defined as follows:

$$P : \Sigma \to \Sigma, \quad \Sigma = \{(x(t), \dot{x}(t)) | t = 0, 2\pi/\Omega_2, 4\pi/\Omega_2, \ldots\} \subseteq R^2.$$

One hundred initial points are randomly chosen on the phase plane. For each initial point, after deleting the first 500 transients, the succeeded 1500 iteration points are plotted by using fourth-order Rutter–Kutter method solving Eq. (1). From Fig. 3 we can see that the system (1) is chaotic motion for $\omega_0 = 1.0$, $\varepsilon = 0.1$, $\mu = 3.0$ $\alpha = 0.1$, $\gamma = 6.0$, $\Omega_1 = 2.0$, $\beta = 1.0$, $\Omega_2 = 2.0$.

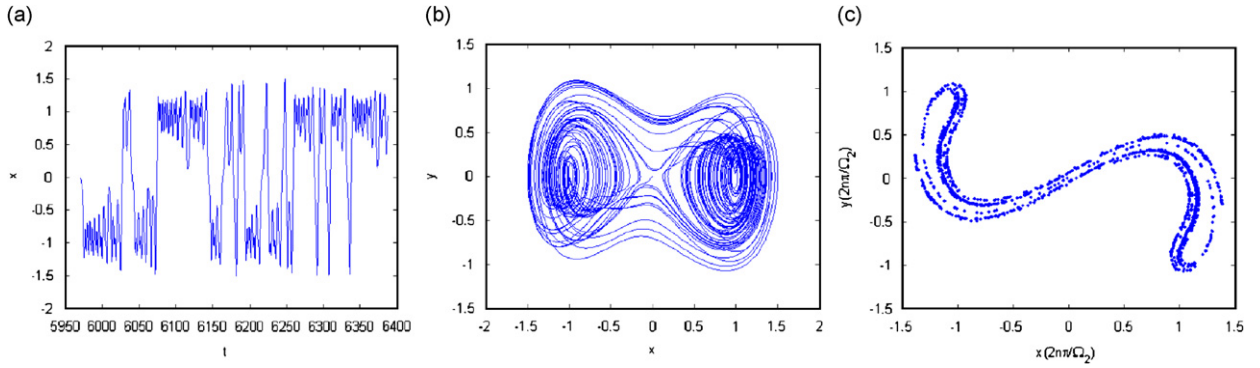

Fig. 4. The chaotic response and Poincaré map of system (1) with $\sigma = 0$, $\delta = 0$: (a) chaotic response; (b) phase portrait; and (c) Poincaré map.

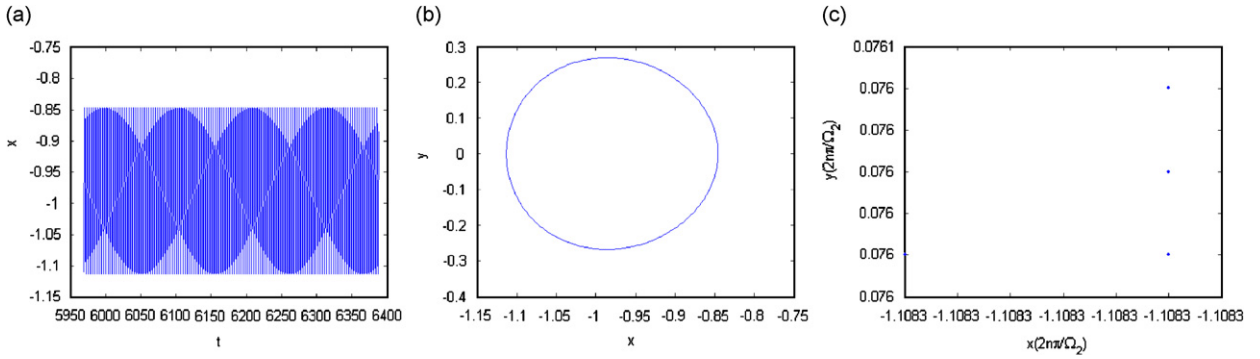

Fig. 5. The chaotic response and Poincaré map of system (1) with $\sigma = 3.0$, $\delta = 0$: (a) chaotic response; (b) phase portrait; and (c) Poincaré map.

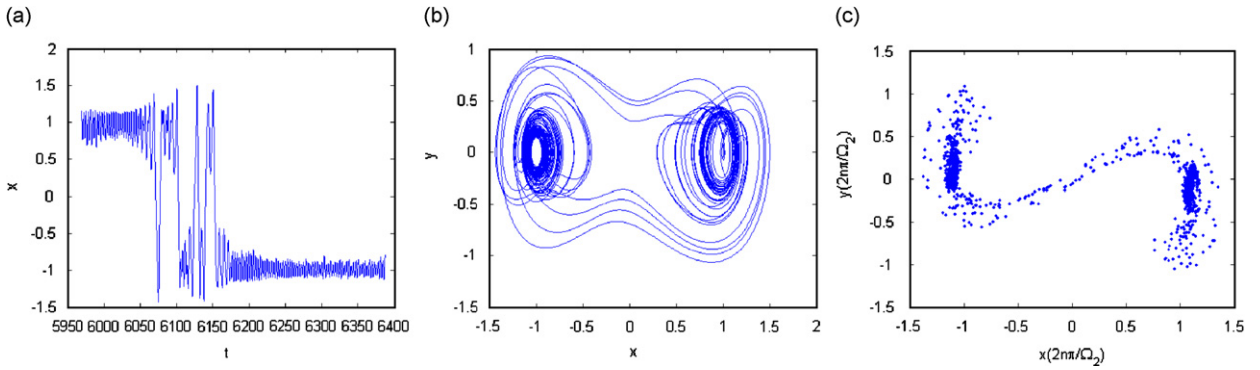

Fig. 6. Chaotic responses and Poincaré map of system (1) with $\sigma = 0.1$, $\delta = 0.1$: (a) chaotic response; (b) phase portrait; and (c) Poincaré map.

So these parameter values are selected for plotting the chaotic response and Poincaré map for some different noise intensity values and the different amplitudes and the results are shown in from Fig. 4(a)–(c) to Fig. 9(a)–(c).

From Figs. 4 and 5, one can see that in the absence of noise, the excitation is harmonic. For the trivial excitation amplitude, the Poincaré map looks like a lying letter 'S' and the motion of the system is chaotic.

While the noise amplitude increases to 3.0, the Poincaré maps are three points and the motion of the system is periodic. It can also be verified by Fig. 3(a).

From Figs. 6 to 9, when the noise present in the system, one can see that for larger noise intensity, the Poincaré maps diffuse larger in phase plane. And then increasing the noise amplitude σ, the Poincaré maps diffuse to a large area, which is the same as a ball in phase plane. In short, the chaotic attractors diffuse by increasing the bounded noise.

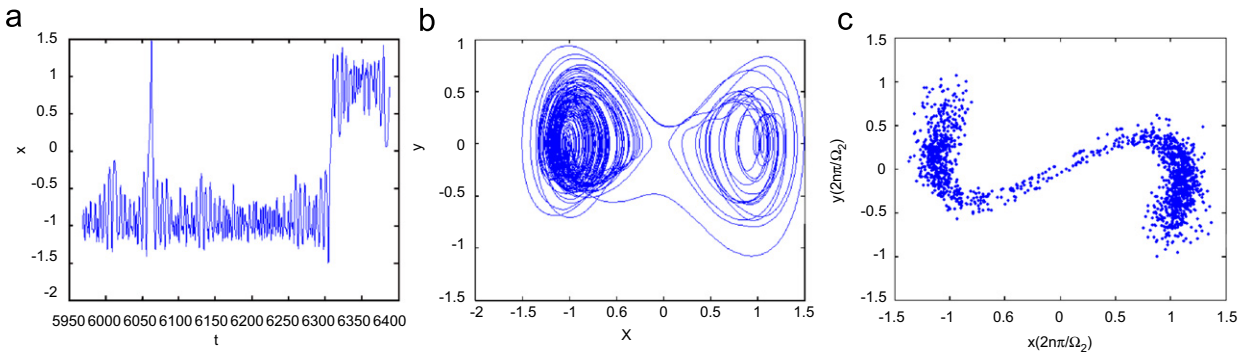

Fig. 7. Chaotic responses and Poincaré map of system (1) with $\sigma = 0.1$, $\delta = 1.0$: (a) chaotic response; (b) phase portrait; and (c) Poincaré map.

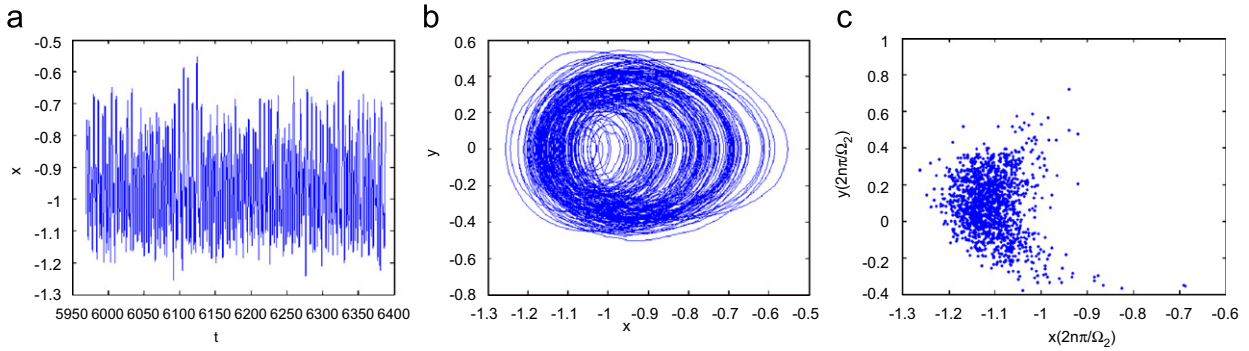

Fig. 8. Chaotic responses and Poincaré map of system (1) with $\sigma = 0.1$, $\delta = 3.0$: (a) chaotic response; (b) phase portrait; and (c) Poincaré map.

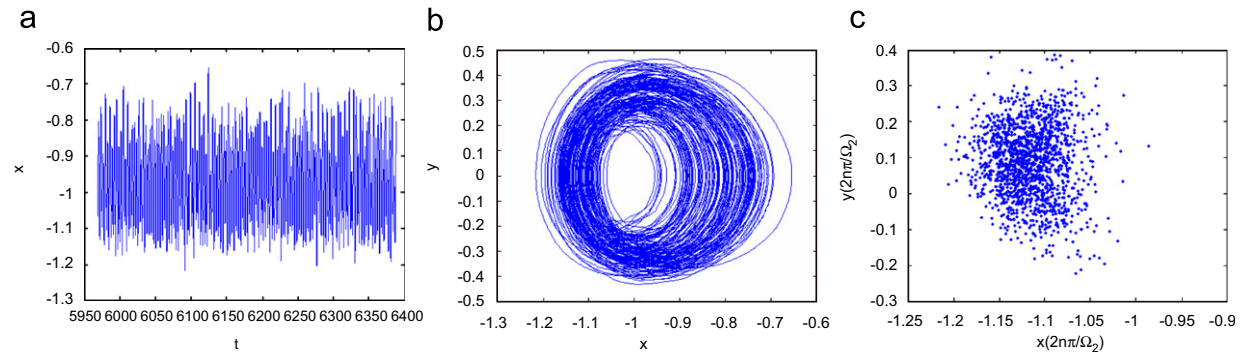

Fig. 9. Chaotic responses and Poincaré map of system (1) with $\sigma = 1.0$, $\delta = 3.0$: (a) chaotic response; (b) phase portrait; and (c) Poincaré map.

5. Conclusions

In the present paper, the chaotic behavior of Van der Pol–Mathieu–Duffing oscillator under bounded noise is investigated in detail by the random Melnikov method with the associated mean-square criterion. The results show that the bound noise can enhance the largest Lyapunov exponent and diffuse the chaotic attractor. The chaotic motion of the Van der Pol–Mathieu–Duffing system can be enhanced by the bounded noise, which is further verified by Poincaré map.

Acknowledgement

This work was supported by the National Natural Science Foundation of China (Grant no. 10472091) and NSF of Shaanxi Province (2003).

References

[1] Y.S. Chen, J. Xu, The Universal classification of principal parametric resonance bifurcation solution of Van der Pol–Duffing–Mathieu type system, *Science in China (series A)* 25 (12) (1995) 1287–1297 (in Chinese).
[2] A.C.J. Lou, Chaotic motion in the generic separatrix bands of a Mathieu–Duffing oscillator with a twin-well potential, *Journal of Sound and Vibration* 248 (3) (2001) 521–532.
[3] A.C.J. Lou, Chaotic motion in the resonant separatrix bands of a Mathieu–Duffing oscillator with a twin-well potential, *Journal of Sound and Vibration* 273 (3) (2004) 653–666.
[4] L. Ng, Bifurcations in a Mathieu equation with cubic nonlinearities, *Chaos, Solitons and Fractals* 14 (2002) 173–181.
[5] L. Ng, R. Band, Bifurcations in a Mathieu equation with cubic nonlinearities, *Communications in Nonlinear Science and Numerical Simulation* 7 (Part II) (2002) 107–121.
[6] J. Li, W. Xu, et al., Maximal Lyapunov exponent and almost-sure stability for Stochastic Mathieu–Duffing Systems, *Journal of Sound and Vibration* 286 (2005) 395–402.
[7] W.Y. Liu, W.Q. Zhu, Z.L. Huang, Effect of bounded noise on chaotic motion of duffing oscillator under parametric excitation, *Chaos, Solitons and Fractals* 12 (2001) 527–537.
[8] C. Gan, Noise-induced chaos and basin erosion in softening Duffing oscillator, *Chaos, Solitons and Fractals* 25 (2005) 1069–1081.
[9] P.J. Holmes, A nonlinear oscillator with a strange attractor, *Philosophical Transactions of the Royal Society* A292 (1979) 419–448.
[10] M. Frey, E. Simiu, Noise-induced chaos and phase space flux, *Physica D* 63 (1993) 321–340.
[11] S. Wiggins, *Global Bifurcations and Chaos: Analytical Methods*, Springer, New York, 1988.
[12] A. Wolf, J.R. Swift, H.L. Swinney, J.A. Vastano, Determing Lyapunov exponents from a time series, *Physica D* 16 (1985) 285–317.